DTA095A - Lab 2 Report

ISTA Deblurring: Pixel vs. Multi-Level Wavelet Sparsity / Plug-and-Play ADMM for Pixel-wise Inpainting / ADMM Inpainting with Explicit Regularizers

Name: Andrea Faccioli
Date: 29/09/2025

1 Introduction

This laboratory session investigates advanced image restoration methods, focusing on deblurring and inpainting problems through optimization-based and Plug-and-Play frameworks. The study examines the performance of the Iterative Shrinkage-Thresholding Algorithm (ISTA) when applied in both the pixel and wavelet domains, highlighting the impact of different sparsity representations on reconstruction quality. Additionally, the Alternating Direction Method of Multipliers (ADMM) is explored for pixel-wise inpainting, incorporating both explicit regularizers and learned denoising priors. The objective of the work is to evaluate how various forms of sparsity, regularization, and prior models influence image fidelity, convergence behavior, and robustness under noise and data loss conditions.

2 Experimental Setup

The experiments have been carried out using **Python** within a **Jupyter Notebook** environment. Core libraries included **NumPy** for numerical operations, **Torch** for tensor-based computations and GPU acceleration, and **scikit-image** for image manipulation and **Deepinv** for pre-trained DRUNet weights. All scripts and functions are provided in Appendix A.1.

3 Results and Analysis

3.1 ISTA Deblurring Pixel vs. Multi-Level Wavelet Sparsity

In this experiment we compared ISTA applied directly in pixel space with ISTA that enforces sparsity in the wavelet domain, across different blur kernels and noise levels. The results show that pixel-space ISTA excels at low noise levels, consistently achieving higher PSNR across all kernel sizes and standard deviations, meaning it reconstructs sharper images when the corruption is mild. However, under high noise ($\sigma = 0.05$), pixel ISTA deteriorates severely, with PSNR values dropping dramatically (e.g., down to 14–16 dB), and LPIPS indicating poor perceptual quality. In contrast, wavelet ISTA is more robust to noise, maintaining stable performance and outperforming pixel ISTA at higher noise, especially in LPIPS, which better reflects visual similarity. For larger blur kernels and higher noise, wavelet sparsity provides a clear advantage, preventing over-smoothing and preserving structures that pixel ISTA fails to recover. Overall, pixel ISTA is preferable in low-noise conditions, but wavelet ISTA generalizes better to challenging noise and blur regimes, making it a more reliable choice in realistic deblurring scenarios.

3.2 Effect of J and lam_wavelet hyperparameters

We now analyze the effect of the wavelet decomposition level J and the regularization weight λ_{wavelet} on ISTA performance. For both noise levels, the results show that the choice of λ_{wavelet} has only a minor influence: PSNR and LPIPS values remain nearly unchanged when varying λ_{wavelet} from 0.001 to 0.05, suggesting that the algorithm is relatively insensitive to this hyperparameter. In contrast, the decomposition level J plays a much larger role. At low noise ($\sigma = 0.01$), the best results are obtained with shallow decompositions ($J = 1$), while deeper decompositions ($J = 2, 3$) tend to degrade performance, especially for larger λ_{wavelet}, where PSNR drops and LPIPS increases. At higher noise ($\sigma = 0.05$), however, a moderate decomposition ($J = 3$) achieves the best trade-off, producing the highest PSNR (22.01) and lowest LPIPS (0.57), showing improved robustness to noise. Overall, the findings suggest that while λ_{wavelet} is not a critical parameter, the decomposition depth J strongly affects performance, with small J preferable at low noise and deeper J beneficial under noisy conditions.

Table 1: Deblurring results: Pixel ISTA vs Wavelet (best values in bold)

Kernel Size	Kernel Std	σ	PSNR Obs	LPIPS Obs	PSNR Pixel ISTA	LPIPS Pixel ISTA	PSNR Wavelet ISTA	LPIPS Wavelet ISTA
7	1.5	0.01	26.14	0.22	**27.61**	**0.24**	25.35	0.27
7	1.5	0.05	23.36	0.46	16.72	0.72	**23.47**	**0.40**
7	3.0	0.01	24.10	0.30	**25.91**	**0.35**	23.13	0.37
7	3.0	0.05	22.15	0.53	14.64	0.87	**21.69**	**0.50**
7	5.0	0.01	23.65	0.30	**25.66**	**0.35**	23.35	0.38
7	5.0	0.05	21.86	0.55	14.10	0.90	**21.51**	**0.52**
15	1.5	0.01	25.96	0.22	**27.63**	**0.23**	25.29	0.28
15	1.5	0.05	23.25	0.47	16.66	0.68	**23.37**	**0.40**
15	3.0	0.01	22.27	0.40	**25.42**	**0.31**	22.65	0.44
15	3.0	0.05	20.89	0.66	20.15	**0.60**	**20.36**	0.65
15	5.0	0.01	20.66	0.48	**24.00**	**0.39**	22.26	0.53
15	5.0	0.05	19.65	0.75	18.77	0.79	**20.60**	**0.74**
25	1.5	0.01	25.96	0.22	**27.62**	**0.23**	25.29	0.28
25	1.5	0.05	23.25	0.47	16.65	0.68	**23.37**	**0.41**
25	3.0	0.01	22.16	0.40	**25.46**	**0.30**	22.65	0.44
25	3.0	0.05	20.80	0.66	20.17	**0.60**	**20.27**	0.66
25	5.0	0.01	19.82	0.54	**22.91**	**0.43**	21.75	0.55
25	5.0	0.05	18.97	0.81	20.47	0.63	**20.69**	0.72

Table 2: Wavelet ISTA performance for different decomposition levels J and wavelet L1 weights λ_{wavelet} (results rounded to two decimals).

$\sigma = 0.01$

J	λ_{wavelet}	PSNR	LPIPS
1	0.001	24.72	0.30
1	0.010	24.70	0.30
1	0.050	24.70	0.30
2	0.001	24.13	0.40
2	0.010	22.64	0.44
2	0.050	22.64	0.44
3	0.001	24.37	0.37
3	0.010	22.04	0.49
3	0.050	20.89	0.54

$\sigma = 0.05$

J	λ_{wavelet}	PSNR	LPIPS
1	0.001	20.67	0.64
1	0.010	20.62	0.65
1	0.050	20.62	0.65
2	0.001	21.30	0.63
2	0.010	20.31	0.66
2	0.050	20.30	0.66
3	0.001	22.01	0.57
3	0.010	21.60	0.55
3	0.050	20.77	0.57

3.3 Effect of LL shrinkage

An additional experiment compared the effect of applying shrinkage also to the LL (low–low) subband of the wavelet decomposition. The LL band mainly encodes the coarse approximation and global structure of the image, and therefore is typically not assumed to be sparse. As expected, shrinking LL coefficients led to a slight decrease in PSNR (as shown in Figure 1), indicating that useful structural information was being suppressed. While this operation may attenuate very low-frequency noise, the trade-off comes at the cost of oversmoothing and reduced fidelity. Even if the performance loss isn't accentuated, it's common practice not to shrink LL subband.

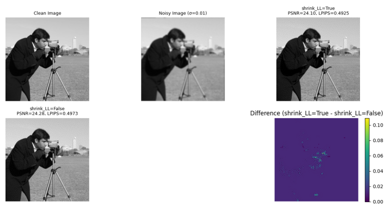

Figure 1: Effect of LL shrinkage

4 Plug-and-Play ADMM for Pixel-wise Inpainting

In this experiment, we assess the performance of many different methods for the inpainting of images characterized by various levels of noise and amount of masked pixels. Overall, DRUNet achieves the best balance between fidelity (highest PSNR) and perceptual quality (lowest LPIPS) across all noise levels and missing ratios, demonstrating the effectiveness of deep denoising priors when integrated in the Plug-and-Play ADMM framework. An overview of the performance of each denoiser is reported in Table 3

It's interesting to highlight the the effectiveness of Nearest Neighbor filling, especially at moderate noise level and low noise (Figure 2), overperforming median, bilateral and Non-local means denoisers.

Median denoiser is instead drastically failing at higher amounts of inpainted pixels (Figure 3).

Table 3: Comparison of inpainting methods for different missing ratios p and noise levels σ. Each cell shows PSNR [dB] / LPIPS (↓ lower is better). Best values are highlighted in bold.

Method	$p = 20\%$			$p = 50\%$			$p = 80\%$		
	$\sigma = 0.000$	$\sigma = 0.010$	$\sigma = 0.050$	$\sigma = 0.000$	$\sigma = 0.010$	$\sigma = 0.050$	$\sigma = 0.000$	$\sigma = 0.010$	$\sigma = 0.050$
Zero-fill	12.13 / 1.0237	12.13 / 1.0260	12.01 / 1.0696	8.20 / 1.1734	8.19 / 1.1745	8.16 / 1.2020	6.15 / 1.1865	6.14 / 1.1873	6.14 / 1.2074
NN-fill	31.21 / **0.0782**	30.71 / 0.0934	25.25 / 0.3124	27.35 / 0.1720	27.14 / 0.1854	23.92 / 0.3836	24.02 / 0.3018	23.92 / 0.3109	22.10 / 0.4826
Median	26.84 / 0.1032	26.81 / 0.1050	25.98 / 0.1771	25.31 / 0.1562	25.40 / 0.1568	24.83 / 0.2061	5.19 / 0.9541	5.19 / 0.9543	5.19 / 0.9565
Bilateral	19.03 / 0.5607	18.99 / 0.5636	19.11 / 0.5585	18.46 / 0.5281	18.45 / 0.5342	18.31 / 0.5493	15.92 / 0.5986	15.92 / 0.6003	15.86 / 0.6225
NLM	27.69 / 0.1151	27.63 / **0.1148**	26.34 / 0.1416	24.67 / 0.2234	24.63 / 0.2235	23.92 / 0.2469	21.08 / 0.4057	21.06 / 0.4066	20.73 / 0.4408
DRUNet	**33.24** / 0.0867	**33.08** / 0.0872	**30.30** / **0.0906**	**30.70** / **0.1163**	**30.59** / **0.1163**	**28.69** / **0.1218**	**26.21** / **0.1992**	**26.15** / **0.2002**	**25.19** / **0.2161**

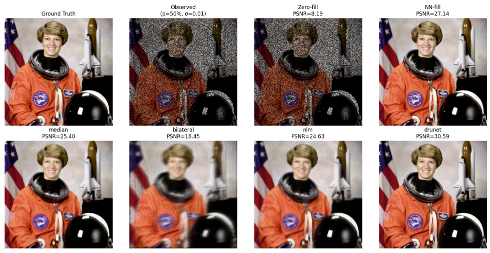

Figure 2: Comparison of different denoisers results for $p = 50\%$ and $\sigma = 0.01$

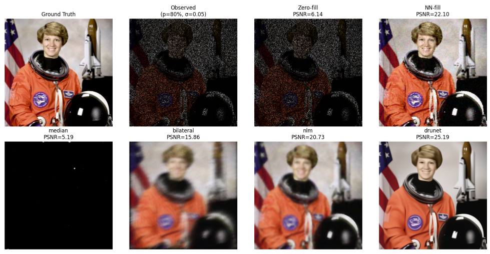

Figure 3: Comparison of different denoisers results for $p = 80\%$ and $\sigma = 0.05$

All the denoisers have been executed with $num\_iterations = 40$. This number has been proved to be sufficient for all of them. DRUNet has shown to have a slower convergence compared to the other three tested methods. Its higher computational cost has been traded off for better performance in all the tested settings. A fine tuning of the strength parameter of the DRUNet denoiser is essential to avoid oversmoothing the images. $strength = 0.3$ has shown great results and has been used for the seek of this session.

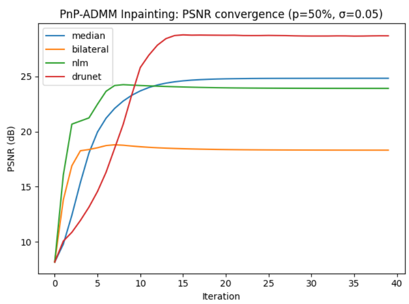

Figure 4: Convergence chart for $p = 50\%$ and $\sigma = 0.05$

5 ADMM Inpainting with Explicit Regularizers

The ADMM experiment with explicit regularizers reveals clear differences in reconstruction quality across regularizers and regularization strengths. DRUNet and Total Variation (TV) achieved the best performance, with optimal PSNR values of 33.65 dB and 32.79 dB respectively, and very low LPIPS scores, indicating visually faithful reconstructions. Tikhonov (gradient) also performed reasonably well, while Tikhonov (identity) consistently yielded poor results, suggesting it fails to impose meaningful spatial regularity.

In Figure 7 the results of the inpainting using different regularizers can be visually assessed: DRUNet is providing a clear and detailed final estimate, preserving edges and consistently removing artifacts. Total

Table 4: ADMM Reconstruction Results for Different Regularizers and λ Values

Method	$\boldsymbol{\lambda}$	**PSNR (dB)**	**LPIPS**
drunet	0.05	13.63	0.8614
	0.08	17.02	0.5406
	0.12	33.65	0.0571
tv	0.02	32.79	0.0492
	0.05	28.18	0.1044
	0.10	24.58	0.1896
tikh_identity	0.005	12.15	1.0298
	0.010	12.14	1.0297
	0.050	12.05	1.0352
tikh_grad	0.20	30.05	0.0672
	0.50	26.83	0.1367
	1.00	24.60	0.2133

variation and Gradient-tikhonov tend to over-smooth the image, especially with higher `lambda` values. Identity-tikhonov regularization is struggling to identify and reconstruct inpainted pixels.

In Figure 5 the PSNR curves for different regularizers have been reported: DRUNet is taking significantly more iterations to reach the plateau compared to the others.

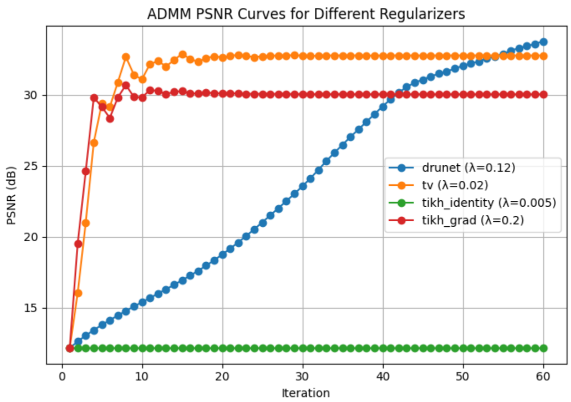

Figure 5: Convergence chart for different regularizers

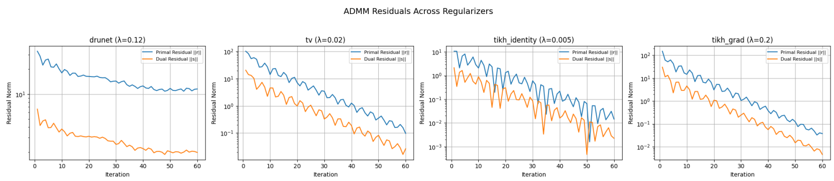

Figure 6: Primal and dual residuals plot

6 Conclusion

The experiments demonstrated that enforcing sparsity in the wavelet domain improves robustness to noise and blur compared to pixel-domain ISTA, particularly in challenging conditions. Inpainting experiments using ADMM confirmed the effectiveness of learned priors such as DRUNet, which achieved the best balance between fidelity and perceptual quality, but at a higher computational cost. Overall, the results highlight the advantages of combining optimization-based frameworks with data-driven denoisers, providing a powerful and flexible approach to modern image restoration tasks.

A Appendix

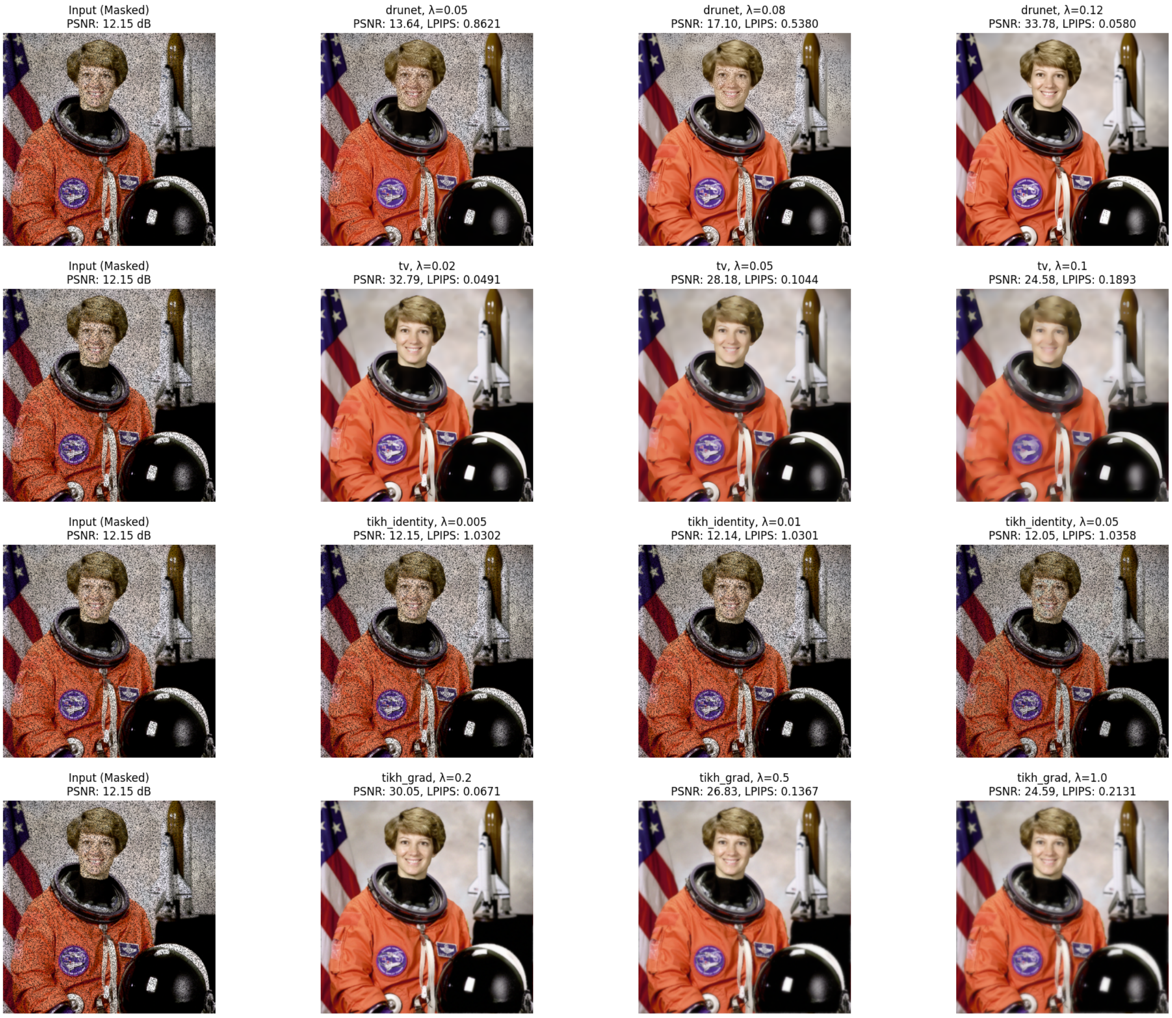

Figure 7

A.1 Source code and images

The complete code and the images processed in Lab2 session can be found here.